Supporting Information

Ag_2S-$AgInS_2$: p-n junction heteronanostructures with quasi Type-II band alignment

Riya Bose, Goutam Manna, Santanu Jana and Narayan Pradhan**

Centre for Advanced Materials and Department of Materials Science, Indian Association for the Cultivation of Science, Kolkata- 700032, India

Experimental Section

Materials

Silver (I) acetate (Ag(OAc), 99.99%), Indium (III) acetate ($In(OAc)_3$, 99.99%), Sulfur (S powder), Oleylamine (OAm, tech.), Octadecene (ODE, tech.) were purchased from Aldrich. All the chemicals were used without further purification.

Synthesis of $AgInS_2$-Ag_2S heterostructures

In a typical synthesis, 0.1 mmol $In(OAc)_3$ (0.032g) was taken in a three necked flask along with 5 mL oleylamine (OAm) and 1 mL ODE. The mixture was degassed by purging argon for 10 min. Then the temperature was increased to 200 ^oC to dissolve $In(OAc)_3$. Once a clear solution was obtained, the temperature was cooled down to room temperature and 0.1 mmol Ag(OAc) (0.016 g) was added into the flask. Then it was again degassed by purging argon for 10 min. After degassing, the temperature was increased to 180 ^oC and annealed for 10 min. Then 0.25 mmol S powder (0.008 g) dissolved in 0.5 mL ODE was injected into the flask and the temperature was increased to 210 ^oC. At that temperature, it was annealed for another 10 min. Then the temperature was cooled down and samples were collected.

Purification

The as synthesized nanocrystals were precipitated using excess acetone from the crude product and further purified using chloroform as solvent and acetone as non-solvent. The purified nanocrystals were dispersed in chloroform for further measurements.

Instrumentation

Optical measurements: Agilent-8453 UV-vis spectrophotometer and Varian-cary-5000 UV-vis-NIR were used for UV-vis and NIR measurement respectively.

Transmission electron microscopy (TEM): TEM images were taken with a JEOL-JEM 2010 electron microscope using 200 kV electron source and a UHR-FEG-TEM, JEOL; JEM 2100

F model using 200kV electron source. Specimens were prepared by dropping a drop of nanocrystal solution in chloroform on a carbon coated copper grid, and the grid was dried in air. TEM images on STEM (HAADF) mode were taken in the UHR-FEG-TEM.

Scanning tunneling microscopy (STM) and scanning tunneling spectroscopy (STS): For STM & STS studies, the dilute solution of sample in chloroform was deposited by drop cast technique on freshly cleaved HOPG substrate by means of mechanical exfoliation. After drying the sample in an oven, it was further heated at ~150 ^{o}C for 30 min inside the glovebox to deplete the ligands on the surface. FTIR spectra of the sample before and after annealing have been provided in Figure S7. After that, it was immediately inserted into the load lock chamber of the STM (Omicron UHV STM). After overnight pumping of the load lock chamber, the sample was inserted into the main STM chamber. All STM measurements were carried out at 2×10^{-10} Torr pressure. The bias voltage and set current during scanning were 2V and 0.5 nA respectively.

X-ray diffraction (XRD): XRD of the samples were taken by Bruker D8 Advance powder diffractometer, using Cu Kα (λ= 1.54 Å) as the incident radiation.

Device fabrication for photovoltaic measurement: For device fabrication, ITO coated glass substrate was cleaned by detergent, de-ionized water, acetone, methanol and finally with 2-propanol. In each step, the substrate in the cleaning solution was sonicated in an ultrasonic bath for 15 min. Finally the substrate was dried in vacuum oven at temperature of 120 ^{o}C. At first, a 15 nm PEDOT:PSS (Baytron P 4083) layer was spun on ITO substrate at a speed of 5000 rpm. PEDOT:PSS film was annealed at 150 °C for 15 min on a hot plate. Then a chloroform solution of the purified $AgInS_2$-Ag_2S heterostructures with concentration of 20 mg/mL was spin coated on the substrate at a speed of 2000 rpm for 60s. The film was then heated to 150 ^{o}C for 30 min to remove excess solvent and then cooled down to room temperature. Finally, a 100 nm film of Silver (Ag) as strip orthogonal to ITO electrodes was

thermally evaporated under vacuum (~10^{-6} Torr). Overlap of ITO and Ag strips defined the area of the devices (4 mm^2). After silver evaporation, the devices were further annealed at 150 °C for 20 min under inert atmosphere.

Current-Voltage (I-V) measurement: I-V characteristics under dark and illumination conditions were recorded with a Keithley 6517B Electrometer. The photocurrent was measured by illuminating the samples with white light of intensity 100 mW/cm^2. A 150 W Newport-Stratfort Solar Simulator model 76500, attached with an AM 1.5 filters, acted as the source for illumination.

Formation mechanism of $AgInS_2$-Ag_2S heterostructures:

To understand the formation mechanism of the heterostructures, we analysed the TEM images of the intermediate samples collected during successive stages of the reaction. Figure S2(a-b) show the TEM images obtained from the sample collected after dissolution of $In(OAc)_3$ in (OAm+ODE) mixture and before addition of Ag which show In_2O_3 agglomerated nanostructures. Formation of In_2O_3 nanostructures under similar reaction conditions has already been reported in literature.[1] XRD of the sample also shows peaks corresponding to cubic In_2O_3 (Figure S2c). Samples collected at 10 min after Ag(OAc) addition and prior to S injection show formation of several larger size particles along with the unchanged In_2O_3 agglomerated nanostructures (Figure S2(d-e)). Figure S2f shows the XRD pattern of this sample which shows peaks corresponding to cubic Ag(0) along with cubic In_2O_3. So the larger size particles are nothing but Ag(0) nanoparticles. Formation of Ag(0) nanoparticles is expected by reduction of Ag(I) in presence of amine.[2] However, in the XRD of the final sample (Figure S1) no peak corresponding to Ag(0) is observed which rules out the presence of Ag(0) in the final nanostructures.

The formation of the heterostructures via In_2O_3 and Ag(0) nanoparticles was further confirmed from the successive absorbance spectra obtained from stepwise collected samples (Figure S3a). After dissolution of $In(OAc)_3$ in OAm, the absorption bandedge is obtained at ~390 nm which matches well with the band gap of cubic In_2O_3 (~3 eV),[3] whereas after Ag(OAc) addition to the reaction mixture and annealing, an additional sharp absorbance peak was obtained at ~410 nm. This is the typical absorbance for surface plasmonic resonance of Ag(0) which suggests that Ag(0) nanoparticles have been formed in the reaction medium.[4] Finally, after S injection, the Ag(0) surface plasmonic absorbance is completely diminished and the band edge shifts to ~670 nm indicating formation of $AgInS_2$. This again rules out the presence of Ag(0) in the final nanostructures. The final sample also shows another absorption bandedge in the near–IR region (~1100 nm) (Figure S3b) which originates due to the Ag_2S part.

So, after S injection to the reaction mixture containing In_2O_3 agglomerated nanostructures and Ag(0) nanoparticles, these $AgInS_2$-Ag_2S heterostructures are formed. As Ag has a higher affinity towards S, soon after addition of S, Ag_2S is formed first. We also confirmed this by injecting S-precursor to the solution containing only agglomerated In_2O_3 nanostructures at the same temperature and annealing (~180 ^oC-210 ^oC), where In_2S_3 formation was not observed. Ag-chalcogenides are known to be superion conductors where the high mobility of Ag^+ promotes a lot of Ag^+ vacancies in the nanocrystals. This high density of cation vacancies in turn promotes foreign cation incorporation.[5] Hence, once Ag_2S is formed in the reaction medium, In^{3+} ions diffuse into it to form $AgInS_2$ species, which in turn is pushed out from Ag_2S and locates on a suitable lattice plane of Ag_2S with minimized lattice mismatch. So Ag_2S acts here as catalyst to form $AgInS_2$ by acting as a host for In^{3+} ions as well as serves as the source material for formation of $AgInS_2$.[5a]

Supporting Figures

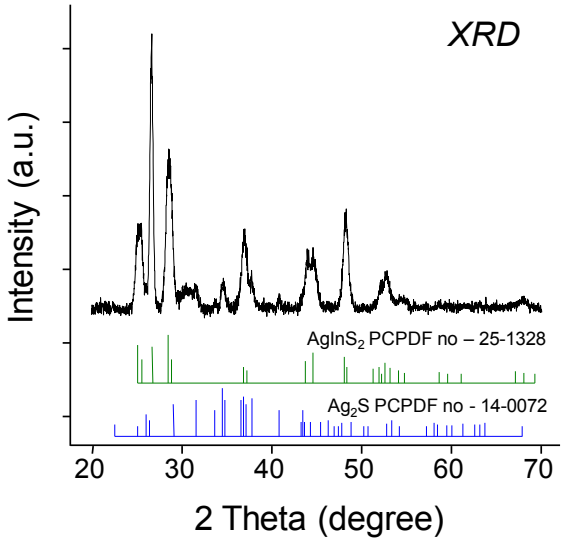

Fig. S1. XRD of $AgInS_2$-Ag_2S heterostructures which shows peaks corresponding to orthorhombic $AgInS_2$ and monoclinic Ag_2S.

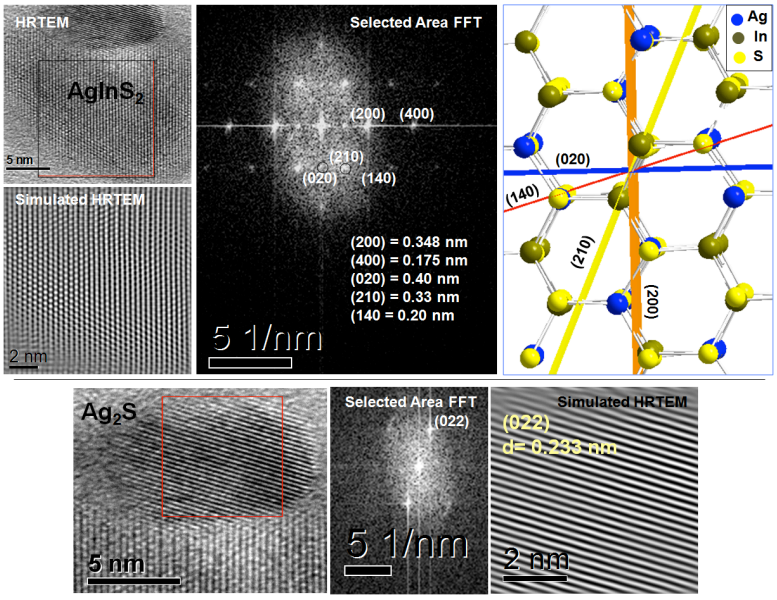

Fig. S2. Upper Panel: HRTEM image, Simulated HRTEM, Selected area FFT pattern and correlated atomic model of $AgInS_2$ part of the heterostructure. Bottom Panel: HRTEM image, FFT and simulated HRTEM of Ag_2S part of the heterostructures. The planes are marked for both cases and these are self-explanatory.

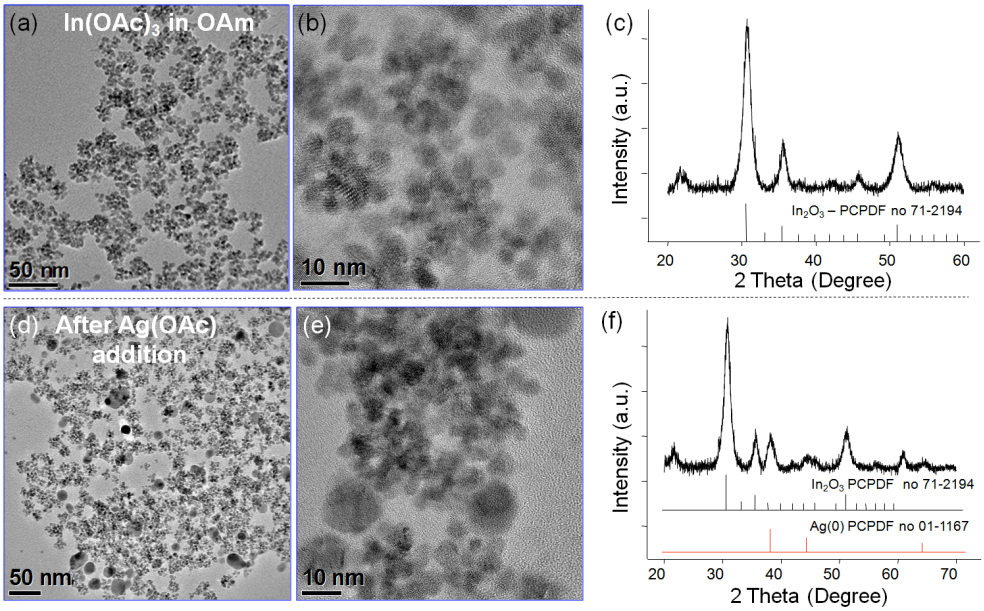

Fig. S3. (a-b) TEM and HRTEM image of the sample collected after dissolution of $In(OAc)_3$ in (OAm+ODE) and before addition of Ag(OAc), which show formation of agglomerated In_2O_3 nanostructures. (c) XRD of the same which shows peaks corresponding to cubic In_2O_3. (d-e) TEM and HRTEM image of the sample collected after Ag(OAc) addition to the reaction mixture and annealing for 10 min. Large Ag(0) nanoparticles are observed along with In_2O_3 nanostructures. (f) XRD of the sample which shows peaks corresponding to cubic In_2O_3 and cubic Ag(0).

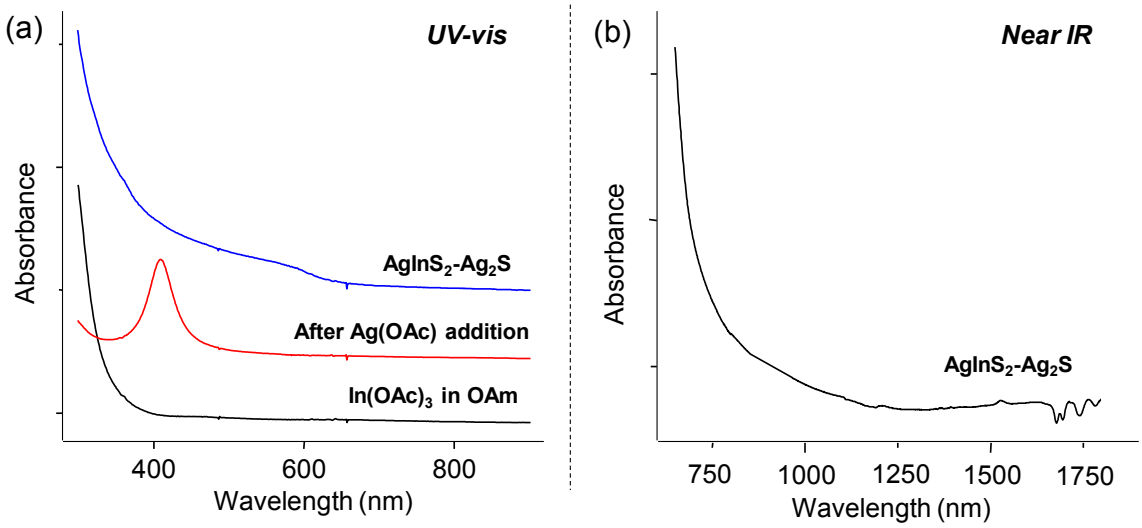

Fig. S4. (a) Successive UV-vis absorbance spectra during the formation of $AgInS_2$-Ag_2S heterostructure. (b) Absorbance spectrum of the heterostructures in near-IR region which shows absorption bandedge at (~1100 nm) originating due to the Ag_2S part.

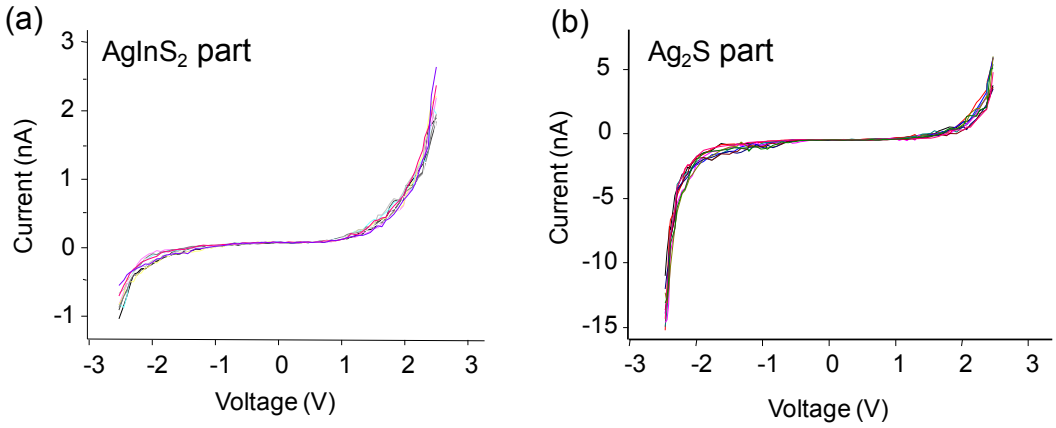

Fig. S5. Current vs voltage plot obtained from scanning tunnelling spectroscopy measurement by placing the STM tip over $AgInS_2$ part (a) and Ag_2S part (b) respectively.

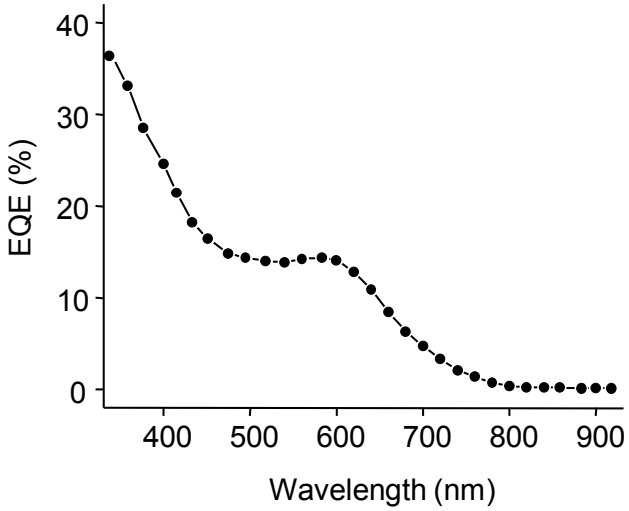

Fig. S6. External quantum efficiency (EQE) spectrum of ITO/PEDOT:PSS/Ag_2S-$AgInS_2$/Ag device under white light illumination. The spectrum shows its maxima at ~600 nm and it matches quite well with the absorbance spectra of the heterostructures. It is also observed that the response of the device is higher in the visible region than in the NIR region.

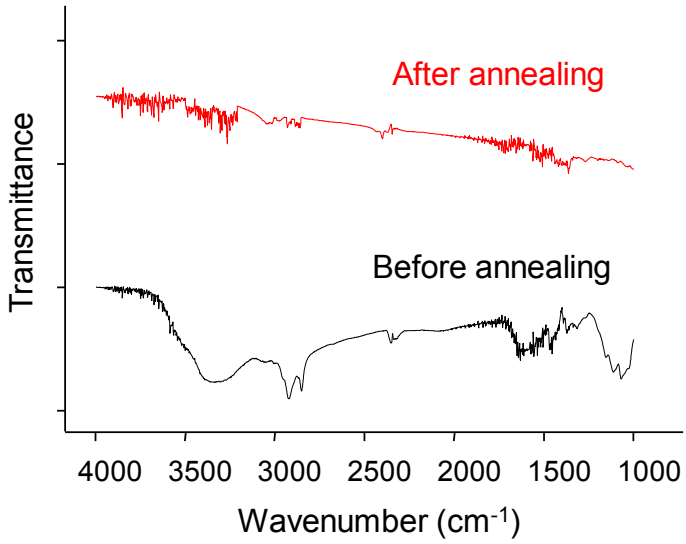

Fig. S7. FTIR spectra of $AgInS_2$-Ag_2S sample before and after annealing before STM measurement. The bands around 3200-3500 cm^{-1} correspond to $–NH_2$ stretching, 2920 and 2852 cm^{-1} correspond to methyl stretching and the bands around ~1330-1700 cm^{-1} correspond to $–NH_2$ bending mode, all of which appears due to presence of oleylamine as a ligand on the surface on the heterostructures. On the other hand, after annealing, the intensity of all the

signals are markedly reduced which indicates that the surface ligands have been successfully depleted.

1 A. Narayanaswamy, H. Xu, N. Pradhan, M. Kim, X. Peng, *J. Am. Chem. Soc.* 2006, **128**, 10310-10319 .
2 D. Wang, T. Xie, Q. Peng, Y. Li, *J. Am. Chem. Soc.* 2008, **130**, 4016-4022.
3 P. D. C. King, T. D. Veal, F. Fuchs, C. Y. Wang, D. J. Payne, A. Bourlange, H. Zhang, G. R. Bell, V. Cimalla, O. Ambacher, R. G. Egdell, F. Bechstedt, C. F. McConville, *Phys. Rev. B* 2009, **79**, 205211/1-205211/10.
4 Q. Zhang, J. Xie, J. Yang, J. Y. Lee, *ACS Nano* 2008, **3**, 139-148.
5 (a) G. Zhu, Z. Xu, *J. Am. Chem. Soc.* 2011, **133**, 148-157; (b) J. Wang, K. Chen, M. Gong, B. Xu, Q. Yang, *Nano Lett.* 2013, **13**, 3996-4000